Vol 18 No 6, June 2009
1674-1056/2009/18(06)/2383-06

Chinese Physics B

© 2009 Chin. Phys. Soc.
and IOP Publishing Ltd

Fabrication of high-quality three-dimensional photonic crystal heterostructures*

Liu Zheng-Qi(刘正奇), Feng Tian-Hua(冯天华), Dai Qiao-Feng(戴峭峰), Wu Li-Jun(吴立军), and Lan Sheng(兰 胜)†

Laboratory of Photonic Information Technology, School for Information and Optoelectronic Science and Engineering, South China Normal University, Guangzhou 510006, China

(Received 24 October 2008; revised manuscript received 20 November 2008)

Three-dimensional photonic crystal (PC) heterostructures with high quality are fabricated by using a pressure controlled isothermal heating vertical deposition technique. The formed heterostructures have higher quality, such as deeper band gaps and sharper band edges, than the heterostructures reported so far. Such a significant improvement in quality is due to the introduction of a thin TiO_2 buffer layer between the two constitutional PCs. It is revealed that the disorder caused by lattice mismatch is successfully removed if the buffer layer is used once. As a result, the formed heterostructures possess the main features in the band gap of constitutional PCs. The crucial role of the thin buffer layer is also verified by numerical simulations based on the finite-difference time-domain technique.

Keywords: photonic crystal heterostructure, pressure controlled isothermal heating vertical deposition, finite-difference time-domain technique

PACC: 4270Q, 7320A, 6185

1. Introduction

Photonic crystals (PCs) formed by the periodic modulation of the dielectric constant have been intensively and extensively studied in the last two decades due to their potential applications in the construction of various functional devices.[1−3] Particularly, three-dimensional (3D) PCs with complete band gaps are highly desirable in practical application, and so various techniques have been developed.[4,5] Among these techniques, the self-assembled method appears to be an effective and economic way to fabricate 3D PCs.[6,7] The monodisperse particles suspended in a solution are assembled into an ordered structure, i.e. a 3D colloidal PC, generally by capillary or convective force. Since the monodisperse particles usually used in the self-assembled PCs are made from silica or polymer, the 3D colloidal PCs obtained in this way possess only a directional band gap because of the low contrast ratio of their refractive index to air's. Although a complete band gap is unavailable in these 3D PCs, they still attract much attention due to their unique advantages over other PCs. For example, 3D colloidal PCs self-assembled from polystyrene (PS) spheres have been successfully employed to construct ultrafast all-optical switches due to the large nonlinear coefficient of the polymer.[8−10]

From the viewpoint of device application, however, it is necessary to selectively introduce defects with different fashions into perfect PCs to realize various functions such as cavities, waveguides, etc.[11−16] For self-assembled colloidal PCs, various methods have been proposed to create defect modes whose resonant frequencies can be tuned in the band gaps.[17−20] Meanwhile, PC heterostructures[21−26] generated by combining two PCs with different lattice constants and PC superlattices[27,28] created by alternatively repeating two PCs have also been demonstrated. In PC heterostructures, two band gaps appear at different frequencies determined by the lattice constants of the two constitutional PCs. Apparently, such PC heterostructures may offer more flexibility and functionality in practical devices. For instance, two signal lights with different frequencies can be simultaneously or selectively switched off through the pumping of a PC heterostructure with a control light. This

*Project supported by the National Natural Science Foundation of China (Grant No 10674051), the Program for Innovative Research Team of the Higher Education of Guangdong Province, China (Grant No 06CXTD005), and the Key Program of Extracurricular Research in South China Normal University (SCNU), China (Grant No 08GDKC02).

†E-mail: slan@scnu.edu.cn

can be realized by deliberately choosing the frequencies of the signal lights which are usually near the band edges. Therefore, how to fabricate 3D PC heterostructures with high quality has become a key issue to be solved before practical application. A survey of the literature reveals, however, that the achievement of high-quality 3D PC heterostructures with deep band gaps and sharp band edges remains a challenge.[21−27] In order to realize high-quality PC heterostructures, one has to deal with two issues. One is to improve the quality of the constitutional PCs and the other is to modify the interface where lattice mismatch occurs. While the former is closely related to the self-assembled technique that has been employed to fabricate the 3D PCs, the latter relies on the elimination of lattice mismatch occurring at the interface. In the present paper, we report on the realization of high-quality PC heterostructures with deep band gaps and sharp band edges. To achieve this goal, we employ a pressure controlled isothermal heating vertical deposition (PCIHVD) technique developed recently to fabricate PC heterostructures.[29] In addition, we intentionally introduce a thin buffer layer between the two constitutional PCs to solve the problem of lattice mismatch.

2. Fabrication of 3D PC heterostructures by using the PCIHVD technique

So far, self-assembled techniques in different fashions have been employed to fabricate 3D PCs. The refinement of the fabrication technique has enabled the quality of the 3D PCs to be improved by reducing defects, dislocations and stacking faults introduced in the fabrication process. Recently, Zheng *et al* [29] demonstrated high-quality 3D PCs with deep band gaps and sharp band edges by using a PCIHVD technique. The key point of this technique is to control the evaporation rate of the solution through accurately controlling the ambient pressure and temperature. In this way, an abrupt band edge with a maximum value of differential transmission $\mathrm{d}T/\mathrm{d}\lambda$ (as large as 7%/nm) has been achieved. This sharp band edge is quite crucial in realizing all-optical switch with a low switching power. By slightly modifying the experimental setup, we have succeeded in obtaining high-quality 3D PCs whose differential transmissions are further enhanced to 10%/nm.[30] In the present work, the modified PCIHVD technique is used to fabricate 3D PCs and heterostructures. Thus, the quality of the constitutional PCs is guaranteed and we can focus on the quality of the interface between them.

In experiment, two types of PS spheres (Duke Scientific Corp.) with diameters of 260 nm and 360 nm were used to synthesize the 3D PCs which are denoted as A and B in the following. The dispersion of PS spheres was less than 3% and their refractive index was about 1.59. For comparison, four samples were fabricated on glass substrates. They were individual 3D PCs (A and B), a PC heterostructure formed by the direct growth of crystal B on crystal A (denoted as AB), and a PC heterostructure with a thin buffer layer between the two PCs (denoted as ATB). Here, T refers to a thin TiO_2 layer of about one hundred nanometers in thickness, which served as a buffer layer between crystals A and B. The synthesis of 3D colloidal PCs was carried out in the same way as that reported previously where optimum experimental conditions were determined.[30] The concentration of PS spheres in the solutions was chosen to be 0.5 wt.%. The pressure in the vial was set at 45 mmHg and the temperature was kept at 35 °C during the fabrication of crystal A. Then, the pressure in the vial was reduced to 40 mmHg and the temperature was increased to 37 °C to fabricate crystal B into the PC heterostructure. As for heterostructure AB, it was obtained by directly depositing crystal B on crystal A which had been dried at room temperature for about 24 h to enhance its mechanical strength. Differently, a thin TiO_2 layer was spin-coated on crystal A and dried at room temperature for about 12 h prior to the deposition of B in the fabrication of the heterostructure ATB. Its thickness was controlled by adjusting the concentration of TiO_2 and/or the speed of the spin coating. Here, we choose T-L series TiO_2 (Solaronix Swiss) with an average size of about 37 nm and a concentration of 1 wt.% for the fabrication of the TiO_2 layer. In addition, the rate of spin coating was set at 1800 rpm per minute.

3. Characterization of 3D PC heterostructures

Scanning electron microscope (SEM) was used to examine the morphology of the PC heterostructures, especially their cross sections. The ordering of PS spheres inside the constitutional PCs and the stack-

ing faults of the PS layers can be easily identified from the SEM images. In addition, transmission measurements were utilized to characterize the quality of the PC heterostructures by focusing on the transmission in the pass bands, the depth of the band gaps and the sharpness of the band edges.

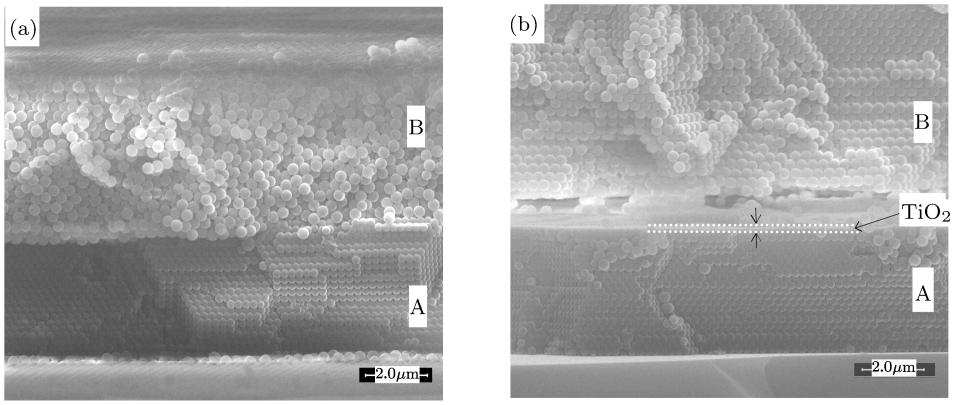


Fig.1. SEM images for the cross sections of PC heterostructures AB (a) and ATB (b).

The SEM images for heterostructures AB and ATB are shown in Figs.1(a) and 1(b), respectively. A significant difference in the ordering of the PS spheres is found in crystal B. In heterostructure AB, PS spheres are no longer stacked layer-by-layer in crystal B due to lattice mismatch occurring at the interface, resulting in many defects and dislocations. In sharp contrast, the layer-by-layer stacking of PS spheres remains in crystal B of heterostructure ATB. It indicates that the thin TiO_2 layer, which is observed between the two PCs, plays a crucial role in determining the quality of the formed heterostructures. In the heterostructure ATB, the thin TiO_2 layer uniformly coated on crystal A acts as a new planar substrate with a smooth surface which ensures the layer-by-layer growth of crystal B on its top by vertical deposition.[31] In other words, the existence of crystal A has no effect on the preparation of crystal B with the addition of the thin TiO_2 buffer layer. Consequently, the disorder formed in crystal B of the heterostructure AB disappears completely because of the elimination of the lattice mismatch at the interface.

The transmission spectra for the individual PCs (A and B) and for the PC heterostructures (AB and ATB) are presented in Figs.2(a) and 2(b), respectively. The thicknesses of the individual PCs are the same as those in the PC heterostructures. For both PCs (A and B), we observe a high transmission over 80% in pass bands, indicating the low volume density of imperfections inside the PCs. A transmission difference as large as about 65% is observed in the band gaps of both samples. The maximum differential transmission is estimated to be about 5%/nm for sample A and about 3.6%/nm for sample B. In Fig.2(b), two band gaps are clearly observed in the transmission spectra of heterostructures AB and ATB. The central wavelengths of the band gaps are coincident with those of the corresponding PCs. However, the main features of the band gaps (e.g. shape, depth, sharpness, etc.), which reflect the quality of the formed PC heterostructures, are modified more or less as compared with those in the individual PCs. It is noticed that a significant modification of the band gap corresponding to crystal B is found in heterostructure AB. In comparison, the change in the band gap, originating from crystal A, is relatively small. It is also remarkable that for heterostructure ATB the modifications in the two band gaps are much smaller, indicating that the quality of the constitutional PCs is similar to that of the individual PCs. It implies that the introduced thin TiO_2 layer successfully isolates the two PCs and eliminates the "cross talk" caused by lattice mismatch at the interface. A detailed comparison between heterostructures AB and ATB will be presented in the next section.

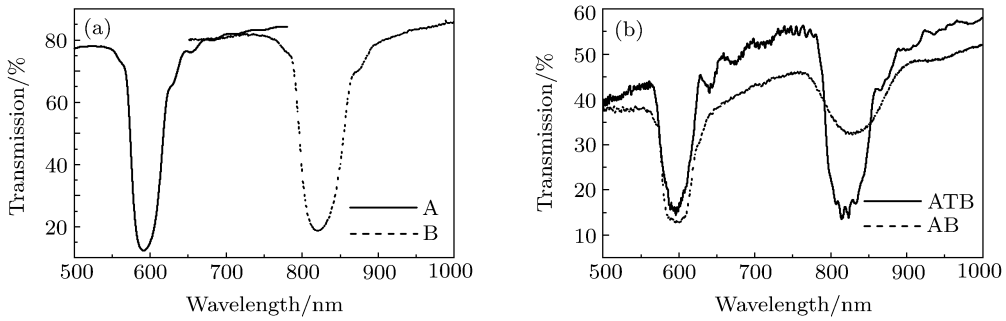


Fig.2. Transmission spectra of individual PCs (A and B) (a) and PC heterostructures (AB and ATB) (b).

4. Effects of the TiO_2 buffer layer on the quality and optical property of 3D PC heterostructures

Now we come to compare the detailed features of the band gaps in the two heterostructures, including the band gap depth, the transmission in the pass bands and gaps, and the differential transmission at the band edges. For heterostructure AB, the depths of the band gaps corresponding to crystals A and B are estimated to be about 25.5% and around 13.8% respectively. The transmission in the pass bands is reduced from about 80% to around 40% as compared with that of the individual PCs. Apparently, the band gap related to crystal B is dramatically reduced and broadened, indicating that the quality of crystal B in heterostructure AB is greatly deteriorated as compared with that of the individual PC. As evidenced in the SEM image, the large lattice mismatch (∼32%) at the interface is responsible for the degradation of crystal quality. While a maximum differential transmission is still observed to be about 2.5%/nm at the band edge of crystal A, it decreases dramatically to only 0.5%/nm at the band edge of crystal B.

When a thin TiO_2 layer was spin-coated on crystal A, the lattice mismatch between the two PCs is completely eliminated and crystal B with a highly ordered structure was successfully grown on crystal A. The resulting heterostructure ATB exhibits a high quality which is manifested in deep band gap and sharp band edge. The transmission in the pass band between the two gaps reaches about 56% which is close to the value anticipated from an ideal heterostructure (80%×80%=64%). In addition, the depth of the band gap corresponding to crystal A exceeds 31% while that originating from crystal B reaches 43.5%. The band gap depth corresponding to crystal B is observed to greatly increase (about 30%) compared with that of heterostructure AB. In contrast, the increase in band gap depth is only ∼5% for the band gap corresponding to crystal A. Besides, Fabry–Perot (F-P) fringes are observed in the pass band between the two gaps and in the long-wavelength pass band of heterostructure ATB. These F-P fringes originate from the interference of the light emerging from the bottom surface and the upper surface of the sample.[7] The appearance of F-P fringes usually indicates that the sample possesses a uniform thickness and a low volume density of defects over the measurement area. In comparison, no F-P fringe is found in heterostructure AB because the coherence of the light emerging from the upper surface is degraded by the disorder present in crystal B.

5. Comparison between experimental measurements and numerical simulations

In order to gain a deep insight into the influence of lattice mismatch and the TiO_2 buffer layer on the quality of the formed heterostructures, we perform 3D numerical simulations for two perfect heterostructures with AB and ATB configurations and compare the simulated transmission spectra with those obtained from experimental measurements. The results are presented in Fig.3. The finite-difference time-domain (FDTD) technique was employed in the numerical simulations.[32,33] In the numerical simulations, the [111] direction of the PCs, which is normal to the glass substrate, was chosen to be the z axis of the coordinate. The grid sizes along the x axis and the y axis

were both set to be 0.0625 μm while that along the z axis was set to be 0.05 μm. A perfectly matched layer boundary condition was employed in the simulations. The number of PS layers for crystals A and B was chosen to be 22, similar to that observed in SEM images.

In Fig.3(a), it is noticed that the band gaps obtained by numerical simulations are much deeper and narrower than those observed in experimental measurements. The difference between these features appears to be more significant for crystal B than for crystal A. It implies that the disorder induced by lattice mismatch greatly deteriorates the quality of crystal B, including both the band gap and the pass bands. The band gap corresponding to crystal A is mainly influenced by the decrease of transmission in the pass bands of crystal B. Another remarkable feature in the simulated transmission spectra is the appearance of F-P fringes in the pass bands. These F-P fringes disappear completely in the measured transmission spectrum of heterostructure AB due to the disorder formed in crystal B.

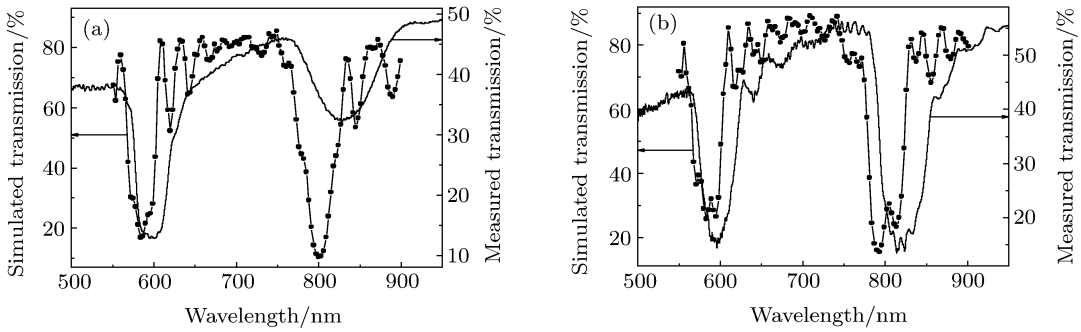


Fig.3. Comparison between measured and simulated transmission spectra for heterostructures AB (a) and ATB (b).

When we compare the simulated and the measured transmission spectra for heterostructure ATB, it is found that the difference in band gap corresponding to crystal B is significantly reduced. Except for a broadening of the band width and a reduction of transmission in the pass bands, the band gap shape appears to be similar in the two cases. It confirms that the introduction of the thin TiO_2 buffer layer is really responsible for the improvement in the quality of the heterostructure.

6. Discussion

So far, the fabrication of PC heterostructures has been reported in several papers.[21−26] No matter how the measurements of reflection or transmission were employed to characterize the properties of the formed heterostructures, the achievement of deep band gaps and sharp band edges remains a challenge. For example, the band gap depths corresponding to crystals A and B for the heterostructure AB were reported to be about 15% and around 18% respectively in Ref.[26]. This value is only half of the band gap depth observed in our heterostructure. In addition, the transmission in the pass band is only 33% which is much lower than that of our heterostructure. Furthermore, the band gaps reported in these papers generally appear to be asymmetric while those observed in our heterostructure are nearly symmetric. In contrast to the results shown in the previous reports,[21−27] clear F-P fringes found in heterostructure ATB implies the high uniformity and less imperfections in our heterostructure. More importantly, the band gaps in our heterostructure possess much sharper band edges with a differential transmission range from 3.5 to 5%/nm as compared with those reported previously. All these features indicate a significant progress in the fabrication of PC heterostructures achieved by using the PCIHVD technique together with a thin TiO_2 buffer layer.

Before summarizing our research work, we show the dependence of the transmission spectrum on the incident angle for heterostructure ATB. Similar to the case of individual PCs, the two band gaps shift toward

shorter wavelengths with the increase of the incident angle. Meanwhile, a reduction of band gap depth is found for both band gaps. Obviously, this reduction occurs more rapidly in the band gap corresponding to crystal B. Both band gaps remain symmetric even at an incident angle of 35°, implying the high-quality of the heterostructure.

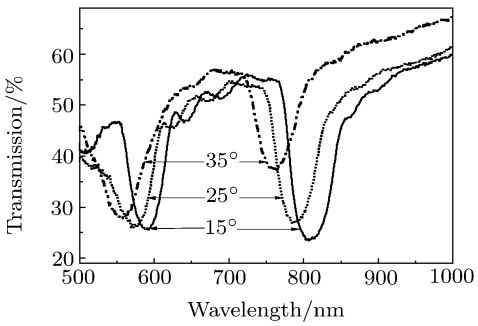


Fig.4. Angle-resolved transmission spectra for heterostructure ATB.

7. Summary

In summary, we have succeeded in fabricating high-quality 3D PC heterostructures with deep band gaps and sharp band edges by using a PCIHVP technique. It is found that the disorder caused by lattice mismatch is successfully removed by introducing a thin TiO_2 buffer layer between the two constitutional PCs. The crucial role of the thin buffer is also confirmed by numerical simulations based on the FDTD technique. The high-quality PC heterostructures reported in this paper may find applications in the construction of some functional devices.

References

[1] Yablonovitch E 1987 *Phys. Rev. Lett.* **58** 2059
[2] John S 1987 *Phys. Rev. Lett.* **58** 2486
[3] Joannopoulos J D, Meade R D and Win J N 1995 *Photonic Crystals: Molding the Flow of Light* (Princeton: Princeton University Press)
[4] Inoue K and Ohtaka K 2004 *Photonic Crystals: Physics, Fabrication, and Applications* (Berlin: Springer-Verlag)
[5] Noda S and Baba T 2003 *Roadmap on Photonic Crystals* (London: Kluwer Acadamic Publishers)
[6] Jiang P, Bertone J F, Hwang K S and Colvin V L 1999 *Chem. Mater.* **11** 2132
[7] Zhou Z C and Zhao X S 2005 *Langmuir* **21** 4717
[8] Hu X Y, Zhang Q, Liu Y H, Cheng B Y and Zhang D Z 2003 *Appl. Phys. Lett.* **83** 2518
[9] Liu Y H, Hu X Y, Zhang D X, Cheng B Y, Zhang D Z and Meng Q B 2005 *Appl. Phys. Lett.* **86** 151102
[10] Wing Y T and Wang X 2006 *Acta Phys. Sin.* **55** 5389 (in Chinese)
[11] Lan S, Nishikawa S and Wada O 2001 *Appl. Phys. Lett.* **78** 2101
[12] Hu X Y, Jiang P, Ding C Y, Yang H and Gong Q H 2008 *Nature Photonics* **2** 185
[13] Lan S, Gopal A V, Kanamoto K and Ishikawa H 2004 *Appl. Phys. Lett.* **84** 5124
[14] Yan Q F, Chen A, Chua S J and Zhao X S 2005 *Adv. Mater.* **17** 2849
[15] Jin C J, Richard M D L R and Nigel P J 2008 *Chin. Phys.* B **17** 1298
[16] Feng Z F, Wang X G, Li Z Y and Zhang D Z 2008 *Chin. Phys.* B **17** 1101
[17] Wostyn K, Zhao Y X, Schaetzen G D, Hellemans L, Matsuda N, Clays K and Persoons A 2003 *Langmuir* **19** 4465
[18] Lee W, Pruzinsky S A and Braun P V 2002 *Adv. Mater.* **14** 271
[19] Tetreault N, Miguez H, Yang M S, Kitaev V and Ozin G A 2003 *Adv. Mater.* **15** 1167
[20] Tetreault N, Mihi A, Miguez H, Rodriguez I, Ozin G A, Meseguer F and Kitaev V 2004 *Adv. Mater.* **16** 341
[21] Jiang P, Ostojic N G, Narat R, Mittleman M D and Colvin V L 2001 *Adv. Mater.* **13** 389
[22] Egen M, Voss R, Griesebock B, Ientel R, Romanov S and Torres C S 2003 *Chem. Mater.* **15** 3786
[23] Li H L and Marlow F 2005 *Chem. Mater.* **17** 3809
[24] Gaponik N, Eychmuller A, Rogach A L, Solovyev V G, Torres Sotomayor C M and Romanov S G 2004 *J. Appl. Phys.* **95** 1029
[25] Bardosova M, Pemble M E, Povey I M, Tredgold R H and Whitehead D E 2007 *Appl. Phys. Lett.* **89** 093116
[26] Nair R V and Vijiaya R 2007 *J. Appl. Phys.* **102** 056102
[27] Rengarajan R, Jiang P, Larrabee D C, Colvin V L and Mittlman D M 2001 *Phys. Rev.* B **64** 205103
[28] Masse P, Pouclet G and Ravaine S 2008 *Adv. Mater.* **20** 584
[29] Zheng Z Y, Liu X Z, Luo Y H, Cheng B Y, Zhang D Z, Meng Q B and Wang Y R 2007 *Appl. Phys. Lett.* **90** 051910
[30] Feng T H, Dai Q F, Wu L J, Guo Q, Hu W and Lan S 2008 *Chin. Phys.* B **17** 4533
[31] Pozas R, Mihi A, Ocana M and Miguez H 2006 *Adv. Mater.* **18** 1183
[32] Sullivan D M 2000 *Electromagnetic Simulation Using the FDTD Method* (Newyork: IEEE)
[33] Taflove A and Hagness S C 1995 *Computational Electrodynamics: The Finite-Difference Time-Domain Method* (Norwood: Artech House Inc.)